

# Dosimetric Implications of Pulmonary Macrophage Clusters Observed within Lungs of Rats That Have Inhaled Enriched $\text{UO}_2$ Particles

by Keith J. Morris,<sup>1</sup> Caroline L. Barker,<sup>2</sup> Angus L. Batchelor,<sup>2</sup> and Paul Khanna<sup>2,3</sup>

Twenty-four Fischer 344 rats were exposed to enriched uranium dioxide ( $\text{UO}_2$ ) aerosols to give a mean initial lung burden of  $291 \pm 89$  (SD)  $\mu\text{g}$ . Groups of rats were killed at 1, 7, 180, 360, 540, and 720 days post-inhalation (PI). Their lungs were fixed and inflated. Sections cut from all five lung lobes were used to prepare CR-39 neutron-induced  $^{235}\text{U}$  fission fragment autoradiographs. A single traverse across a CR-39 autoradiograph of a tissue section, from the left lung of all the rats, was made using a motorized microscopic stage. The traverse was divided into 10 fields. The track counts per field were used to test for homogeneity of track distribution and to assess if there was any tendency for tracks to be related to the peripheral region of the lung. Full raster scans across the entire tissue image were made on left lung autoradiographs from two animals killed at each time point to assess the homogeneity of fission fragment track distribution throughout the entire section. There was no evidence of any temporal change in the proportion of tracks associated with the lung periphery. At all time points PI, the track distribution was significantly nonhomogeneous, suggesting a nonuniform pattern of tissue irradiation from the  $^{234}\text{U}$   $\alpha$  particles.

At time points from 180 to 720 days PI, large clusters of macrophages were observed in some of the sections taken from all five lung lobes. The total number of macrophage clusters increased with time PI. These macrophage clusters produced many  $^{235}\text{U}$  fission fragment tracks within the CR-39 autoradiographs. The tracks within these macrophage clusters represented 0.4%–84% of the entire track count for the section. The mean  $^{234}\text{U}$   $\alpha$ -particle dose rate within these clusters was calculated to be 0.033 and 0.13 Gy/day, depending on the size of the cluster. This compares with the estimated dose rates averaged over the whole lung of 0.021 Gy/day at 4 days PI and 0.0057 Gy/day at 720 days PI.

## Introduction

To satisfactorily assess the radiation dose to lung cells at risk of cancer induction, it is necessary to know the microscopic spatial distribution of the inhaled radioactive particles within the lung tissues. This is particularly important for highly insoluble particles (International Commission on Radiological Protection [ICRP] Class Y), such as plutonium oxide ( $\text{PuO}_2$ ) and uranium dioxide ( $\text{UO}_2$ ) that have long residence times in the lung. Data from animal studies suggest that such particles become increasingly less randomly distributed with time after inhalation (1). In particular, the particles appear to become more associated with the lung periphery and peribronchial tissue (2,3). Diel et al. (4) speculate that this association may be due to preferential clearance of particles from the more central alveolar regions. In

cases of high particle burdens or lung dose, it seems that particles also become associated with fibrotic areas of extensive tissue damage (5).

The principal agent for the clearance and redistribution of particles within the lung is the phagocytic alveolar macrophage. Sanders (6) showed that insoluble  $^{239}\text{PuO}_2$  particles retained in the lung from 1 to 2 days after inhalation were normally in macrophages. Large aggregates of macrophages containing insoluble anthracitic particles have been observed by Cottier et al. (7) in lungs from humans of "advanced age." The particle-laden macrophages were principally associated with pleural and septal lymphatics. Only 2% of all the particles observed in the lung were associated with alveolar tissue. Cottier et al. (7) discuss the relevance of this finding to possible "hot spots" in lung doses after radionuclide inhalation.

This paper presents data from a long-term study of the spatial distribution of inhaled, enriched  $\text{UO}_2$  particles within the lung of the Fischer 344 rat. The work is concerned with the dosimetric importance of clusters of alveolar macrophages observed to be laden with  $\text{UO}_2$  particles. An assessment is made of whether the dose to tissues within the rat lung was likely to have been reasonably uniform over the lung during the 720-day post-

<sup>1</sup>Harwell Biomedical Research, A.E.A. Technology, B.551, The Harwell Laboratory, Oxon OX11 0RA, UK.

<sup>2</sup>M.R.C. Radiobiology Unit, Chilton, Oxon OX11 0RD, UK.

<sup>3</sup>Present address: Plasma Fractionation Laboratory, Churchill Hospital, Headington, Oxford, Oxon OX3 7LT, UK.

Address reprint requests to K. J. Morris, Harwell Biomedical Research, A.E.A. Technology, B.551, The Harwell Laboratory, Oxon OX11 0RA, UK.

inhalation (PI) period. Earlier work with the same lung tissue sections suggested that the central alveoli, subpleural alveoli, and airway tissue regions would receive about the same  $^{234}\text{U}$   $\alpha$ -particle dose over the 720 days PI (8). In this paper the randomness of the  $\text{UO}_2$  particle distribution in the lung is further investigated to discover if the dose within these three lung tissue regions is likely to be uniform or highly uneven. Discussions of other aspects of this  $\text{UO}_2$  particle distribution study are given in Morris et al. (8,9).

## Materials and Methods

### Inhalation Procedure

Twenty-four male Fischer 344 rats were exposed nose-only for 100 min to an aerosol of enriched  $\text{UO}_2$  at a concentration of about  $150 \text{ mg/m}^3$ . A complete description of the exposure procedure for these rats is given by Morris et al. (9). The activity median aerodynamic diameter of the aerosol ranged from 2.7 to  $3.2 \mu\text{m}$ , with a geometric standard deviation of 1.7. This suggests that the median Stokes equivalent diameter of the  $\text{UO}_2$  particles is about  $0.8 \mu\text{m}$ , assuming a  $\text{UO}_2$  density of  $11 \text{ g/cm}^3$ .

The enriched  $\text{UO}_2$  particles had a uranium isotopic composition of 92.8%  $^{235}\text{U}$ , 6.06%  $^{238}\text{U}$ , 0.79%  $^{234}\text{U}$ , and 0.34%  $^{236}\text{U}$ , by mass. This gives an  $\alpha$ -particle activity of about  $1.91 \text{ Bq}/\mu\text{g}$ , with a mean  $\alpha$ -particle energy of 4.7 MeV, due mainly to the presence of  $^{234}\text{U}$ . The total  $\gamma$  emission rate is about 40% of the  $\alpha$  activity. For comparison,  $^{239}\text{PuO}_2$  and  $\text{UO}_2$  of natural isotopic composition (99.275%  $^{238}\text{U}$ , 0.72%  $^{235}\text{U}$ , and 0.005%  $^{234}\text{U}$ ) have  $\alpha$ -particle activities of  $2.027 \times 10^3 \text{ Bq}/\mu\text{g}$  and  $0.02 \text{ Bq}/\mu\text{g}$ , respectively.

At 5 days PI, the mass of enriched  $\text{UO}_2$  retained in the lung was estimated by using a small animal whole-body  $\gamma$  scintillation counter (9). The mean initial burden of all the rats was  $291 \pm 89 \mu\text{g}$  (SD), with the lowest burden at  $136 \mu\text{g}$  and the highest at  $473 \mu\text{g}$ .

### Lung Tissue Fixation

Two rats were killed at 1 and 7 days PI. Further groups of five rats were killed at 180, 360, 540, and 720 days PI. The rats were anesthetized by exposure to 4% halothane and then killed by intratracheal instillation of 1% (weight/volume)  $\text{OsO}_4$  in fluorocarbon FC80,\* at an excess pressure of 15 cm above the thorax. This method was selected because the nonpolar solvent does not mix with aqueous lung fluids and has been shown to fix cells on the airway surfaces (10). The inflated lungs were dissected from the body and all five lobes separated. Each lobe was cut into 3-mm transverse slices and further fixed under vacuum for 1 hr in 0.1 M glutaraldehyde. After fixation, the lungs were stored in 0.1 M sodium cacodylate buffer at  $4^\circ\text{C}$ . The uranium content of each lung was estimated using a  $\gamma$  scintillation counter.

The uranium contents of the trachea and extrapulmonary bronchi, thoracic lymph nodes, internal jugular and posterior cervical lymph nodes, kidneys, liver, spleen, and carcass remainder were determined by delayed neutron analysis. These data have been reported by Morris et al. (9).

\*FC-80 (3M Company) is no longer produced. Fluorocarbon F05910, supplied by Fluorochem Ltd., Dinting Vale Trading Estate, Glossop, Derbyshire, UK, seems to be a suitable replacement.

### Locating $\text{UO}_2$ Particles within the Tissue Section

After scintillation counting, some of the 3-mm lung slices were systematically taken from all of the rats and embedded by the method of Spurr (11). Thirteen lung lobe slices were selected from each rat, 2 from right anterior, median, and cardiac lobes (3rd and 6th slices from the apex), 3 from the right posterior lobe (2nd, 5th, and 8th slices from the apex), and 4 from the left lung (2nd, 5th, 8th, and 11th slices from the apex).

The resin blocks were cut serially by microtome to produce tissue sections of nominally  $5\text{-}\mu\text{m}$  thickness. The sections were placed onto cleaned and gelatin-subbed CR-39 polycarbonate solid state track detector slides obtained pre-cut from Track-Analysis Systems (Bristol University, Bristol, UK) cut to the standard glass microscope size of  $76 \text{ mm} \times 25 \text{ mm} \times 1.5 \text{ mm}$ . Every alternate section was placed onto a standard subbed glass slide and stained with hematoxylin and eosin (H&E). Ten  $5\text{-}\mu\text{m}$  sections were cut from each block.

The CR-39 slides were exposed to thermal neutrons within the HERALD reactor at A.W.E. Aldermaston, UK, to produce  $^{235}\text{U}$  fission fragment autoradiographs for the location of the  $\text{UO}_2$  particles. The mean exposure fluence for all the sections was  $5.3 \pm 0.2 \text{ (SD)} \times 10^{12} \text{ neutrons/cm}^2$ .

After neutron exposure, a  $^{238}\text{Pu}$   $\alpha$ -particle shadow image of the lung section was produced in the CR-39 using the method of Gore et al. (12). This method creates a reasonably good resolution tissue image of the lung section while retaining the neutron-induced  $^{235}\text{U}$  fission fragment tracks. The procedure enabled us to locate  $^{235}\text{U}$  fission fragment track foci within the tissue section (see Figures 1-4). It is assumed that the  $^{235}\text{U}$  remains associated with the insoluble  $\text{UO}_2$  particles and that the number of tracks seen is related to the mass of  $\text{UO}_2$  in the tissue section. A full description of the fission fragment autoradiography technique used for the tissue sections mounted on CR-39 is given by Morris et al. (8).

### Image Analysis of $^{235}\text{U}$ Fission Fragment Autoradiographs

#### Single Traverse across a Section from the Left Lung

To investigate whether the lung sections showed any significant temporal changes in the percentage of tracks associated with the lung periphery, a series of single traverses were made across a selected CR-39  $\alpha$ -image autoradiograph made from a tissue section taken from the slice from the apex of the left lung. This was the 3-mm tissue slice with the largest cut surface area. These traverses were made using a light microscope, at  $160\times$  magnification, equipped with a motorized stage and attached to a Seescan Solitaire plus grey-level image analyzer (Seescan Ltd., Cambridge, UK). The image was captured from the microscope using a high-resolution monochrome Newvicon camera and fed into the Seescan image analyzer via a monochrome monitor. The traverse was taken across the widest part of the left lung section image, approximately from the ventral to the dorsal side of the rat. The single traverse was divided into 10 equal lengths such that the opposite edges of the lung made the beginning and end of the traverse. The height of each of the 10 fields was  $500 \mu\text{m}$ . The width of each field varied between 1000 and  $1500 \mu\text{m}$ ,

depending on the width of the lung section image. The number of fission fragment tracks were then counted within each of the 10 fields. Small foci of tracks were counted by eye. The few large foci of tracks observed were measured by the Seescan image analyzer, where the area of the total track focus was divided by the mean area of a single track to estimate the track number. This was repeated using left-lung eighth slices from each rat at every time point PI. The mean percentage of tracks per field was then calculated for each time PI. A chi-square homogeneity test (13) was applied to the data to see if the distribution of tracks across the traverse differed from that expected with uniform track distribution (i.e., 10% per field).

### Uniformity of Track Distribution throughout Entire Section

We randomly selected two of the CR-39 autoradiographs of sections taken from the eighth 3-mm slice from the apex of the left lung from rats killed at each time point. The CR-39 tissue images were systematically raster scanned with the Seescan image analyzer so that all of the section was viewed with no field overlapping. The field size was  $500 \times 500 \mu\text{m}$ . The track number for each field was counted by eye for small track foci and by the image analyzer for the occasional large track foci, using the total track foci area method described above. There were 4–25 large foci (including track aggregates from macrophage clusters) in each section autoradiograph. The total number of accepted fields scanned per section varied from 450 to 650 fields. All fields within the section where no tissue was seen (mainly inside conducting airways) were discounted. Otherwise all fields were accepted, provided they had some tissue visible. We assumed that the percentage of fields with small fractions of tissue present would have been similar for all section images. A chi-square homogeneity test (13) was applied to the track count data from each section to assess whether the number of tracks present within each field was consistent with a uniform track distribution over the entire section.

### Estimation of Number of Macrophage Clusters within CR-39 Autoradiographs

While scanning some of the CR-39 autoradiographs to obtain data for earlier work (8), it was noticed that occasionally some large foci of  $^{235}\text{U}$  fission fragment tracks were seen. These track aggregates were markedly larger than the normal circular foci of tracks and were made up of many overlying large foci (see Figures 1–4). Studying the adjacent H&E tissue sections led to the conclusion that these track aggregates were caused by clusters of macrophages containing many clearly visible black particles that were assumed to be  $\text{UO}_2$ . As these track aggregates were visually quite striking, an attempt was made to assess their significance on total lung doses.

A single CR-39 autoradiograph from each of the 13 lung slices was fully scanned, and the number of these track aggregates counted. This was repeated for all rats, at all time points, giving a total of 52 lung autoradiographs scanned from the 4 rats killed at 1 and 7 days PI and 260 lung autoradiographs scanned from the 20 rats killed at 180, 360, 540, and 720 days PI. The track aggregates were subclassified into large and small macrophage clusters. Small track aggregates typically consisted of 150–500 tracks, whereas large aggregates contained about 300–2000

tracks. The location of each track aggregate was noted and assigned to either subpleural alveolar, central alveolar, or ciliated airway tissue regions, in the manner of Morris et al. (8). The subpleural alveolar region was taken as all alveolar tissue within  $100 \mu\text{m}$  of the lung periphery.

For some of the left lung autoradiographs the total number of fission fragment tracks within the section was already known (8). This was true for all the autoradiographs from the eighth 3-mm slice from the left lung apex (one section per rat) and for all time points from 1 to 720 days PI (a total of 24 autoradiographs). Using this information, the percentage contribution from the track aggregates to the total tracks counted in these left lung tissue sections, was calculated for each time PI.

## Results and Discussion

### Single Traverse across a Section from the Left Lung

The mean percentage of tracks found within each of the 10 fields per traverse across the left lung autoradiograph is given in Table 1. The results of the chi-square homogeneity test of these data, averaged for all rats per time PI and assuming an expected 10% of all tracks in each field, were 1 + 7 days PI,  $\chi^2 = 20 \pm 9$  (SD); 180 days PI,  $\chi^2 = 37 \pm 23$ ; 360 days PI,  $\chi^2 = 93 \pm 98$ ; 540 days PI,  $\chi^2 = 136 \pm 102$ ; and 720 days PI,  $\chi^2 = 114 \pm 39$ . In all cases the results of the chi-square test showed that the distribution of tracks across the traverse was significantly nonrandom ( $p < 0.001$ ). The results of a  $t$ -test comparing these mean chi-square values showed that the 720 days PI point was significantly higher than the two chi-square mean values measured at 4 (1 + 7) and 180 days PI ( $p < 0.01$ ). There was no significant difference between the mean chi-square values found at 4, 180, 360, and 540 days PI.

The results do not suggest an obvious movement of the particles, in terms of track counts, to the periphery of the lung. The most noticeable feature of the data is that the standard deviations of the means given in Table 1 tend to become larger with increasing time PI. Both this and the chi-square test data suggest that the track distribution throughout the traverse section is becoming increasingly less homogeneous with time PI.

**Table 1. Mean percentage of total tracks counted within each of the 10 fields across one traverse of a left lung section autoradiograph.<sup>a</sup>**

Time PI, days	% of total tracks within each field									
	Peripheral		Central						Peripheral	
	1	2	3	4	5	6	7	8	9	10
1 + 7	10.9 (4.0)	10.5 (1.9)	10.3 (5.8)	5.5 (3.0)	13.5 (7.8)	8.9 (5.2)	13.1 (4.2)	10.7 (3.3)	7.6 (4.9)	9.1 (2.4)
180	13.2 (9.4)	8.1 (2.2)	13.5 (1.8)	10.7 (5.8)	11.0 (7.7)	10.4 (9.4)	8.4 (4.1)	8.0 (5.4)	8.1 (7.7)	8.5 (5.1)
360	7.5 (3.0)	6.7 (2.9)	6.7 (5.3)	8.0 (8.7)	11.4 (5.6)	13.4 (13.6)	11.2 (7.8)	17.8 (22.2)	6.7 (6.3)	10.7 (8.9)
540	14.9 (23.5)	3.9 (2.4)	12.6 (8.7)	18.2 (11.7)	7.5 (5.7)	8.2 (7.8)	7.7 (4.8)	3.9 (3.3)	15.0 (22.1)	8.0 (6.5)
720	11.5 (9.7)	11.1 (7.7)	12.2 (15.5)	6.9 (8.4)	12.4 (13.2)	14.2 (13.8)	8.0 (14.4)	6.8 (8.1)	12.7 (13.5)	4.3 (3.5)

PI, post inhalation.

<sup>a</sup>The height of each field was  $500 \mu\text{m}$ , and the length varied from 1000 to  $1500 \mu\text{m}$ . Each data mean is shown with its standard deviation in parentheses. The mean total number of tracks counted in all 10 fields, at each time point, was 1 + 7 days PI =  $2.367 \pm 0.963$  (SD)  $\times 10^3$ ; 180 days PI =  $1.052 \pm 0.367 \times 10^3$ ; 360 days PI =  $563 \pm 382$ ; 540 days PI =  $305 \pm 82$ ; 720 days PI =  $284 \pm 362$  (where  $n = 5$ ; one autoradiograph from five rats per time point PI).

## Uniformity of Track Distribution throughout Entire Section

The results of the chi-square test for homogeneity of track distribution within an entire CR-39 autoradiograph, produced from the left lung slice from two rats killed at 1, 7, 180, 360, 540, and 720 days PI, were 1 day PI,  $\chi^2 = 1.5 \pm 3.6$  (SD)  $\times 10^3$ ; 7 days PI,  $\chi^2 = 22.9 \pm 5.8 \times 10^3$ ; 180 days PI,  $\chi^2 = 25.8 \pm 8.8 \times 10^3$ ; 360 days PI,  $\chi^2 = 50.8 \pm 30.2 \times 10^3$ ; 540 days PI,  $\chi^2 = 42.0 \pm 29.2 \times 10^3$ ; 720 days PI,  $\chi^2 = 146.4 \pm 163.7 \times 10^3$ . The results of the chi-square test showed that all sections measured had a track distribution that was significantly nonrandom ( $p < 0.001$ ).

The high chi-square value at the 720-day PI point was due to one of the sections, which had two large track aggregates, having a chi-square test value of  $260.0 \times 10^3$ . If all of the  $3.873 \times 10^3$  tracks counted in this autoradiograph had been in one of the 552 fields scanned, the chi-square value would be  $2.1 \times 10^6$ . The section from the other rat killed at 720 days PI had a track homogeneity chi-square value of  $31.0 \times 10^3$ .

A *t*-test of the mean chi-square values given above showed no significant difference between any of the PI points. However the single section from the rat killed at 720 days PI with the chi-square value of  $260.0 \times 10^3$  was found to have a track distribution significantly less homogeneous than that found with the autoradiographs from the 1- and 7-day PI time points ( $p < 0.02$ ). So there is an apparent trend of an increasingly less homogeneous track distribution with time PI. Unfortunately, there was insufficient time to scan more sections, which would have improved the sensitivity of the statistical tests by increasing the degrees of freedom.

## Estimation of Number of Macrophage Clusters within all CR-39 Autoradiographs

Table 2 shows the number of macrophage clusters within each lung tissue region, from all the 13 lung lobe sections taken from each rat killed at 1 to 720 days PI. The number of small and large clusters was found to increase consistently with time PI in the subpleural alveolar and airway tissue regions. The number of clusters in the central alveolar tissue region tended to reach a maximum after 360 days PI, falling slightly by 720 days PI. Morris et al. (8) reported that the  $\text{UO}_2$  particles appeared to clear faster from the central alveolar region than from the subpleural alveolar and ciliated airway region. Thus, fewer, particles will

**Table 2. The number of track aggregates observed within each CR-39 tissue-image autoradiograph.\***

Time PI, days	Alveoli		Pleura		Airways	
	Small	Large	Small	Large	Small	Large
1 + 7	0	0	0	0	7	0
180	16	1	5	5	1	0
360	7	9	5	11	5	1
540	7	3	6	18	5	3
720	8	4	10	19	9	7

PI, post inhalation.

\*In all cases the track aggregates appeared to be due to the clustering of alveolar or interstitial macrophages. The section was divided into the pulmonary regions of central alveolar tissue, alveolar tissue within 100  $\mu\text{m}$  of the lung periphery (subpleural alveoli), and ciliated airway tissue. The number of sections scanned (*n*) from all five lung lobes were: at 1 + 7 days PI, *n* = 52; at 180 days–720 days PI, *n* = 65 for each time point PI.

be available in the central alveolar region for the promotion of macrophage clusters. In general, except for clusters associated with airway tissue, the macrophage clusters appeared to be on the alveolar surface. However, the thickness of the H&E-stained section did not give good resolution at high magnification, which precluded detailed histological analysis. Occasionally, macrophage clusters were clearly seen within lymphatic tissue associated with the alveolar subpleural region, although this was only after 180 days PI. Serious lung disease was not observed in the animals until 720 days PI (9), so this should not be an important factor in the  $\text{UO}_2$  particle distribution at earlier time points.

A typical large macrophage cluster found within the central alveolar tissue region, at 360 days PI, is shown in Figures 1 and 2. A similar large macrophage cluster observed in the subpleural alveolar region at 360 days PI is shown in Figure 3.

At the 1- and 7-days PI time points, all the macrophage clusters within the sections were designated as small, and all were found on the inner airway surface (Fig. 4). These were probably in the process of being cleared by the mucociliary escalator. At later times points, all the macrophage clusters were under the airway epithelium and normally associated with airway lymphatic tissue, suggesting that particles within these interstitial macrophages would be retained in this location for long periods. Morris et al. (8) suggest that the observed  $\text{UO}_2$  distribution pattern will lead to a significant dose to the airway tissue, similar to the accumulated dose received by the central and subpleural alveolar tissue from 4 to 720 days PI. No macrophage clusters were observed to be related to alveoli or airway perivascular tissue.

Table 3 gives the percentage of tissue sections found to contain small and large track aggregates. It can be seen that, even at 720 days PI, the majority of sections, 63%, had no large macrophage clusters and that 45% of sections had no macrophage clusters at all. It should be pointed out that even if sections had no macrophage clusters, at the later times PI the track distribution still appeared to be nonrandom within many of the sections, suggesting that the dosimetric pattern of tissue irradiation will be non-uniform. However, as the distribution pattern changes continuously with time due to alveolar and interstitial macrophage movement, and given the 40  $\mu\text{m}$  range of  $\alpha$  particles in tissue (14), the actual tissue irradiation pattern may be more uniform than suggested by these observations.

The total number of  $^{235}\text{U}$  fission fragment tracks were known for 24 of the 8th left lung slice autoradiographs. Using this information the proportion of tracks originating from the macrophage clusters could be found (Table 4). This gives a guide to the dosimetric significance of the small and large macrophage clusters. It can be seen that at the later PI time points, the number of tracks within clusters can represent a significant proportion of the total tracks counted throughout the section (Table 4). The maximum percentage of tracks present within macrophage clusters ranged from 0 to 0.4% of all tracks throughout the section at 4 (1 + 7) days PI. At 180 days PI this value ranged from 0 to 3.77%, at 360 days PI it ranged from 0 to 40.5%, at 540 days PI it ranged from 0 to 6.9%, and at 720 days the tracks within clusters ranged from 11.0 to 83.9% of the total tracks within the section. Thus, even as early as 360 days PI, macrophage clusters could contain enough  $\text{UO}_2$  particles to represent up to 40% of the relative mass of  $\text{UO}_2$  present within the entire section. All these

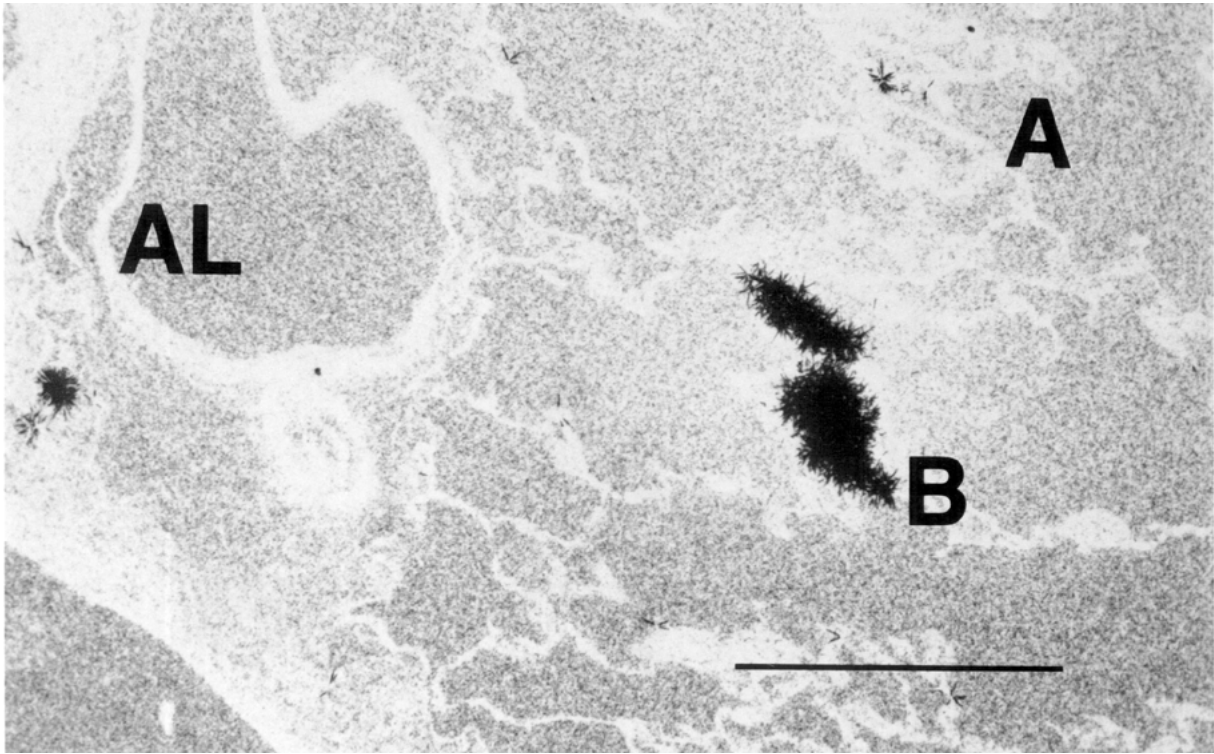


FIGURE 1. A CR-39 autoradiograph of a section from the eighth 3-mm slice from the apex of the left lung of a rat killed at 360 days PI. A large aggregate of  $^{235}\text{U}$  fission fragment tracks can be seen within the central alveolar tissue region. The total number of tracks emanating from the macrophage cluster was estimated to be 750 tracks using the Seescan image analyzer, which represents 18% of the total track count across the section. AL, central alveolar tissue region; A, conducting airway designated as ciliated airway tissue region; B, airway blood vessel designated as ciliated airway tissue region. Bar = 300  $\mu\text{m}$ .

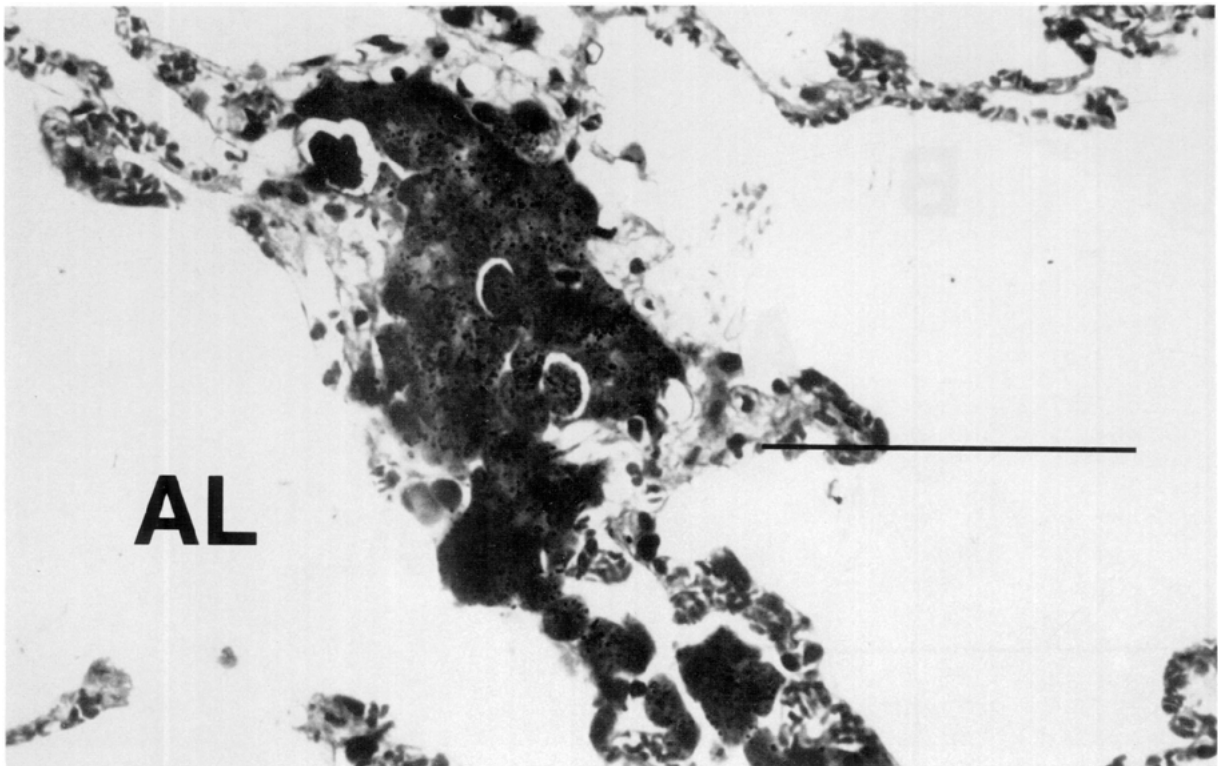


FIGURE 2. Photomicrograph of a hematoxylin and eosin stained section cut serially to the section used to produce the CR-39 autoradiograph shown in Figure 1, although this higher magnification photomicrograph shows the large track aggregate region only. A large alveolar macrophage cluster can be seen, from which the many  $^{235}\text{U}$  fission fragment tracks present in Figure 1 emanate. Particles can be clearly seen within the macrophages, and these are assumed to be enriched  $\text{UO}_2$ . AL, central alveolar tissue region. Bar = 100  $\mu\text{m}$ .



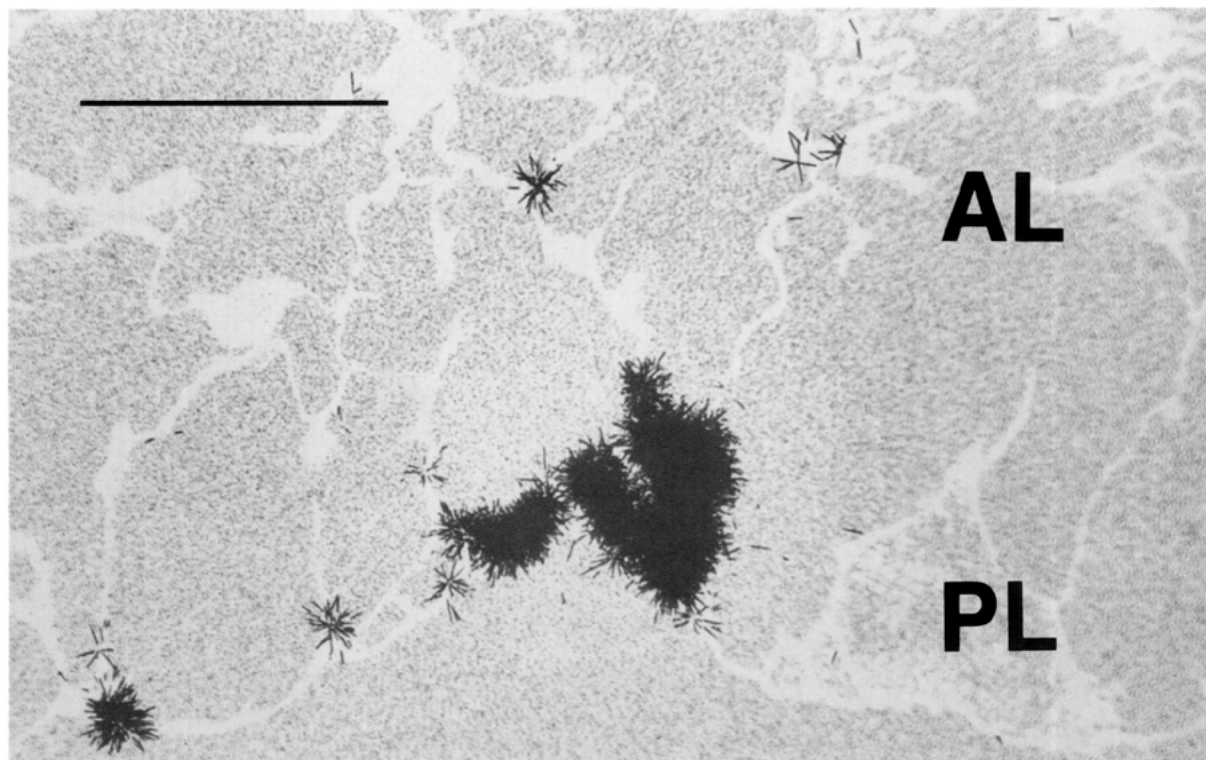


FIGURE 3. A CR-39 autoradiograph of a section from the fifth 3-mm slice from the apex of the right posterior lobe from a rat killed at 360 days PI. A large aggregate of  $^{235}\text{U}$  fission fragment tracks can be seen within the subpleural alveolar tissue region. The total number of tracks emanating from the macrophage cluster was estimated as  $1.4 \times 10^3$  tracks using the Seescan image analyzer. The total section track count was not obtained. AL, central alveolar tissue region; PL, subpleural alveolar tissue region. Bar = 200  $\mu\text{m}$ .

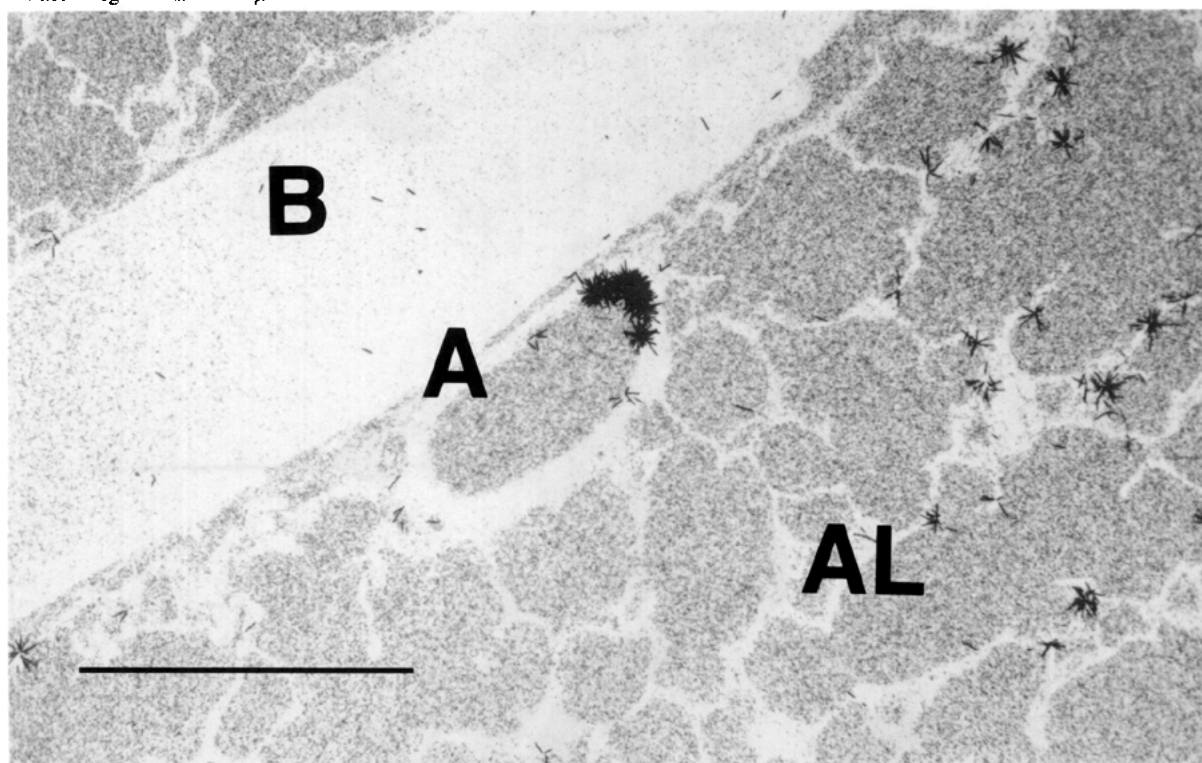


FIGURE 4. A CR-39 autoradiograph of a section from the third 3-mm slice from the apex of the right cardiac lobe of a rat killed at 7 days PI. A small aggregate of  $^{235}\text{U}$  fission fragment tracks can be seen on the surface of a conducting airway, presumably in the process of being cleared via the mucociliary escalator. The total number of tracks emanating from the small macrophage cluster was estimated to be 210 tracks using the Seescan image analyzer. The total section track count was not obtained. AL, central alveolar tissue region; A, conducting airway designated as ciliated airway tissue region; B, airway blood vessel designated as airway perivascular tissue region. Bar = 300  $\mu\text{m}$ .

**Table 3. The number of sections found to have large and small macrophage clusters, expressed as a percentage of the total sections scanned.\***

Time PI, days	% of all sections with			Sections scored
	Small clusters	Large clusters	Both clusters	
1 + 7	11.5	0.0	11.5	52
180	29.2	7.7	36.9	65
360	20.0	23.1	35.4	65
540	21.5	32.3	49.2	65
720	32.3	36.9	55.4	65

PI, post inhalation.

\*The sections were systematically selected from all five lung lobes. For the definition of large and small macrophage clusters, see text.

**Table 4. The proportion of  $^{235}\text{U}$  fission fragment tracks counted within the macrophage clusters.\***

Time PI, days	Sections with clusters, % of section tracks in clusters	All lung sections, % of all tracks in clusters
1 + 7	0.44	0.13
180	2.15	0.49
360	19.70	3.76
540	6.54	1.71
720	37.84	37.84

PI, post inhalation.

\*All measurements were made using CR-39 autoradiographs produced from sections taken from the eighth 3-mm slice from the apex of the left lung. The mean total number of tracks counted within the five left lung section autoradiographs was: 1 + 7 days PI =  $33.690 \pm 11.416$  (SD)  $\times 10^3$ ; 180 days PI =  $16.66 \pm 8.653$   $\times 10^3$ ; 360 days PI =  $5.055 \pm 0.912$   $\times 10^3$ ; 540 days PI =  $3.129 \pm 0.771$   $\times 10^3$ ; 720 days PI =  $2.922 \pm 0.867$   $\times 10^3$ .

particles of  $\text{UO}_2$  would be within a tissue volume (assuming a uniform section thickness) of less than 0.1% of the total tissue volume within the section (8).

However, a lot of sections did not have any macrophage clusters, although they still had comparable numbers of  $^{235}\text{U}$  fission fragment tracks. This fact will reduce the mean percentage of tracks counted within macrophage clusters if related to total sections scored. The second column in Table 4 gives these values. At time points less than 720 days PI, the percentage of tracks within clusters is noticeably lower than the value obtained when only sections with macrophage clusters were considered. At 720 days PI, all sections scored had macrophage clusters, so the values do not change. Given that less than 4% of all tracks were typically associated with clusters at all the time points up to 540 days PI, this suggests that the clusters were not important in terms of the total dose received by the lung over this period. However, the dose rate will obviously be higher to cells within exposure range of the  $\text{UO}_2$  particles inside the macrophage clusters compared to the more uniform  $\text{UO}_2$  distribution throughout the rest of the section. The significance of this higher dose rate is difficult to determine and depends on how important any "hot spot" irradiation is assumed to be in terms of cancer induction. At the later 720-day PI time point, the macrophage clusters clearly have a marked effect on the dosimetric pattern of tissue irradiation, and it appears that the increasingly nonuniform track distribution pattern (as determined by the chi-square test in previous sections) is mainly due to the increase in the number of these macrophage clusters with time PI.

However, by 720 days PI the animals were near the end of their lives, and only about 16% of the initial lung burden was still retained in the lung (9). The animals will have received most of their total lifetime  $^{234}\text{U}$   $\alpha$ -particle dose well before 540 days PI.

By 45, 90, 180, 360, 540, and 720 days PI, the animals were estimated to have received a total  $\alpha$ -particle dose, averaged over the whole lung, of 0.9, 1.6, 2.9, 4.4, 5.2, and 5.7 Gy, respectively (9). Thus the large macrophage clusters observed may have occurred too late in the animals' lives to be important in terms of dose to cells at risk of cancer induction. If the total  $^{235}\text{U}$  fission fragment tracks counted in the eighth left lung slice sections and the total number of tracks counted emanating from macrophage clusters within these sections are plotted against time PI, the area under the curve, from 4 to 720 days PI, is 46 times greater in the case of the total section counts. This suggests that about 2% of all  $^{234}\text{U}$   $\alpha$ -particle emissions occur within the macrophage clusters, and 98% occur within the rest of the lung, over the 720-days PI period. Owing to the increasing number of macrophage clusters observed with time PI, about half of the 2% of  $^{234}\text{U}$   $\alpha$ -particle emissions within clusters appear to be emitted between 540 and 720 days PI. Thus, over the 720-day PI period, by far the greater proportion of cell hits will be from  $\alpha$  particles emitted from  $\text{UO}_2$  located outside the macrophage clusters.

If this were the case, it is possible that the similar clusters of macrophages, all laden with anthracitic particles, which were observed in postmortem human lungs from elderly individuals by Cottier et al. (7), may not have important dosimetric implications. These interstitial macrophage clusters were within pleural and septal lymphatics, not normally the location of macrophages that have recently phagocytized particles from alveolar surfaces. Cottier et al. (7) found few particle-laden macrophages within the human alveoli region of these old individuals. However, as most of the particles seen are likely to have originally come from the alveolar region, the unknown residence times in the human alveoli and latterly in the lymphatic tissue must also be taken into account. Also, the majority of particles inhaled would normally be cleared from the lung over the individuals lifetime (15), either completely from the individual via the mucociliary escalator or, probably to a much lesser extent, to the thoracic lymph nodes (9). It is likely that a substantial part of the total  $\alpha$ -particle irradiation of the lung will come from those particles that clear in such a manner and leave the lung long before lung disease would be clinically detected.

An estimate can be made of the  $^{234}\text{U}$   $\alpha$ -particle dose within the small and large macrophage clusters observed within sections from the eighth left lung slices. As the neutron flux used to produce CR-39 autoradiographs of these sections is known, the mass of  $\text{UO}_2$  within the sections can be calculated (16). It was estimated that one fission fragment track would be expected for every 0.17 pg of  $\text{UO}_2$  after exposure to a thermal neutron fluence of  $5 \times 10^{12}$  neutrons/cm<sup>2</sup>, assuming that all  $^{235}\text{U}$  fissions will result in one track being detected within the CR-39. The tissue area within each individual macrophage cluster was found from alternate H&E sections to that used to produce the autoradiographs. Assuming a uniform section thickness of 5  $\mu\text{m}$ , the approximate tissue volume of each macrophage cluster was calculated, excluding air spaces. The tissue density was taken as 1 g/cm<sup>3</sup>, and the mass of  $\text{UO}_2$  per gram of tissue was calculated. From these values the dose rate within the macrophage clusters was calculated, ignoring all clusters found at 1 and 7 days PI, which were on the airway surface. The dose rate within the small macrophage clusters was estimated to be  $0.033 \pm 0.015$  Gy/day ( $n = 11$ ), and the dose rate within the large macrophage clusters

was estimated to be  $0.130 \pm 0.083$  Gy/day ( $n = 6$ ). In comparison, the dose rate averaged over the whole lung was estimated to be 0.021 Gy/day at 4 days PI, 0.0057 Gy/day at 360 days PI, and 0.0026 Gy/day at 630 days PI (9). If it is assumed that the macrophage clusters remain at the same location within the lung once formed, this suggests the total accumulated dose within small clusters will be 18 Gy over the 180- to 720-day PI period. Similarly, the total accumulated dose within large macrophage clusters would be 47 Gy over the 360- to 720-day PI period. Thus, the local dose to cells intimately associated with the macrophage clusters could be much higher than the estimated accumulated dose of 5.7 Gy averaged over the whole lung from 4 to 720 days PI (9). However, the assumption that these macrophage clusters remain at a fixed location for such long periods may not be valid.

## Conclusions

The distribution of the  $^{235}\text{U}$  fission fragment tracks within the left lung of the rat was found to be nonhomogeneous at all time points from 1 to 720 days PI. This suggests that the pattern of  $^{234}\text{U}$   $\alpha$ -particle irradiation within the lung will be consistently non-uniform throughout the life of the individual after exposure. There was an apparent increase in the nonhomogeneity of the fission fragment track distribution throughout the lung with increasing time PI. Even at the later times PI, there was no evidence that tracks were becoming increasingly associated with the peripheral regions of the lung.

Macrophage clusters were found within many of the rat lung sections taken from all five lobes. The number and size of these clusters increased with time PI. From data taken from the left lung, it appeared that the percentage of tracks associated with these macrophage clusters was less than 4% up to 540 days PI. At 720 days PI, typically 40% of all tracks were counted within these macrophage clusters. This suggests that these macrophage clusters may not be a significant factor in contributing to the total lung dose, as by 540 days PI the rats have received more than 90% of their total accumulated  $^{234}\text{U}$   $\alpha$ -particle lung dose, averaged over the whole lung. However, from 180 to 720 days PI, the estimated dose rate within these macrophage clusters was much higher than the corresponding dose rate calculated by averaging over the whole of the rat lung.

This work was supported in part by the U.K. Department of Energy under contract HM-4-54-64 and by the Commission of the European Communities under

contract B16-D-076-UK. The authors thank Christine Stirling for her technical assistance and advice and Graham Patrick and Leon Cobb for many useful discussions, all of M.R.C. Chilton.

## REFERENCES

1. Swinth, K. L., Goey, P. J., and Rhoads, K. Effects of plutonium redistribution on lung counting. In: *Pulmonary Toxicology of Respirable Particles* (C. L. Sanders, F. T. Cross, G. E. Dagle, and J. A. Mahaffey, Eds.), Technical Information Center, U.S. Department of Energy, Washington, DC, 1980, pp. 224-237.
2. McShane J. F., Dagle, G. E., and Park, J. F. Pulmonary distribution of inhaled  $^{239}\text{PuO}_2$  in dogs. In: *Pulmonary Toxicology of Respirable Particles* (C. L. Sanders, F. T. Cross, G. E. Dagle, and J. A. Mahaffey, Eds.), Technical Information Center, Department of Energy, Washington, DC, 1980, pp. 248-255.
3. Diel, J. H., Mewhinney, J. A., and Snipes, M. B. Distribution of inhaled  $^{238}\text{PuO}_2$  particles in syrian hamster lungs. *Radiat. Res.* 88: 299-312 (1981).
4. Diel, J. H., Mewhinney J. A., and Snipes M. B. Spatial and temporal distribution of  $\text{PuO}_2$  aerosol particles deposited in rodent lungs by inhalation. In: *Lovelace Inhalation Toxicology Research Institute Annual Report for 1978-1979* (R. F. Henderson, J. Diel, and B. S. Martinez, Eds.), LF-69 (UC-48), Lovelace Inhalation Toxicology Research Institute, Albuquerque, NM, 1979, p. 5.
5. Diel, J. H., and Short, R. K. Collagen location in lung parenchyma irradiated by inhaled  $^{238}\text{PuO}_2$  particles. *Radiat. Res.* 79: 417-423 (1979).
6. Sanders, C. L. The distribution of inhaled plutonium-239 dioxide particles within pulmonary macrophages. *Arch. Environ. Health* 18: 904-912 (1969).
7. Cottier, H., Meister, F., Zimmermann, A., Kraft, R., Burkhardt, A., Gehr, P., and Poeretti, G. Accumulation of anthracitic particles along lymphatics of the human lung: relevance to "hot spot" formation after inhalation of poorly soluble radionuclides. *Radiat. Environ. Biophys.* 26: 275-282 (1987).
8. Morris, K. J., Barker, C. L., Batchelor, A. L. and Khanna, P. Temporal variation in the micro-distribution of enriched  $\text{UO}_2$  particles deposited in the left lung of the rat. *Radiat. Prot. Dosim.*, in press.
9. Morris, K. J., Khanna, P., and Batchelor, A. L. Long term clearance of inhaled  $\text{UO}_2$  particles from the pulmonary region of the rat. *Health Phys.* 58: 477-485 (1990).
10. Thursten, R. J., Hess, R. A., Kilburn, K. H. and McKenzie, W. N. Ultrastructure of lungs fixed in inflation using a new osmium-fluorocarbon technique. *J. Ultrastruct. Res.* 56: 39-47 (1976).
11. Spurr, A. R. A new resin embedding technique for lungs. *J. Ultrastruct. Res.* 26: 31-40 (1969).
12. Gore, D. J., Thorne, M. C., and Watts R. H. The visualisation of fissionable radionuclides in rat lung using neutron-induced autoradiography. *Phys. Med. Biol.* 23: 149-154 (1978).
13. Bailey, N. T. J. *Statistical Methods in Biology*. The English University Press Ltd., London, 1964, pp. 67-77.
14. Polig, E. The localised dosimetry of internally deposited alpha-emitters. *Current Top. Radiat. Res.* 13: 189-327 (1978).
15. Stuart, A. E. *The Reticulo-Endothelial System*. Livingstone, Edinburgh, 1970, pp. 3-5.
16. Johns, H. E., and Cunningham, J. R. *The Physics of Radiobiology*, 3rd ed. Charles C. Thomas, Springfield, IL, 1978, pp. 95-98.